Electrical conductivity in the antiferromagnetic insulating phase of V_2O_3

V. N. Andreev and F. A. Chudnovskiy*
Ioffe Physical-Technical Institute, Academy of Sciences of Russia, 194021 St. Petersburg, Russia

J. M. Honig and P. A. Metcalf
Department of Chemistry and School of Materials Engineering, Purdue University, West Lafayette, Indiana 47907, USA
(Received 28 May 2004; published 22 December 2004)

The electrical conductivity of V_2O_3 in the antiferromagnetic insulating (AFI) phase has been measured on multidomain and single-domain crystals over a conductivity range of more than five orders of magnitude, and for the temperature range 160–40 K. The intrinsic mechanism for conductivity in the AFI phase for a single-domain sample of well-defined orientation was determined, using a special experimental setup that minimized mechanical stresses. The conductivity in the AFI phase of the unstressed, single-domain crystal was comparable to the conductivity of the multidomain crystal, but the two samples differ in their temperature dependence. The results were interpreted by analyzing the effect of thermal lattice vibrations on the resonance integral. The polaron localization radius was found to be of the order of the lattice vibration amplitudes.

DOI: 10.1103/PhysRevB.70.235124 PACS number(s): 05.60.−k

I. INTRODUCTION

The present report represents an attempt to demonstrate the variability of results obtained on V_2O_3 with different experimental procedures and to identify a method for overcoming the measurement problems at low temperatures. Pure, stoichiometric V_2O_3 undergoes a paramagnetic metal to antiferromagnetic insulator transition (MIT) with decreasing temperature at ~155 K, accompanied by large changes in physical properties. The electrical resistivity of this compound has been repeatedly investigated,[1–10] yet, at present, there is no agreement concerning the variation of conductivity (σ) with temperature (T) for the low-temperature antiferromagnetic insulating (AFI) phase. Correspondingly, a theory of the electrical properties cannot be constructed until data that establish the actual σ versus T dependence for this phase become available. One problem in obtaining such data is that the resistivity at low T becomes very large (greater than 10^{12} Ω cm) and therefore difficult to measure. Perhaps more important is the fact that the sample fractures in the course of the MIT, resulting in considerable scatter in the experimental data.

II. EXPERIMENTAL

The V_2O_3 crystals used in this study were grown and annealed under carefully controlled conditions described elsewhere.[11] 6-7 mm diam disk-shaped samples of both random and well-defined crystallographic orientations were cut from the single crystals. The randomly oriented samples, 0.1-0.5 mm in thickness, were polished and etched in warm HNO_3. The oriented samples were cut from a plane that coincided with the $(1\bar{1}00)$ crystallographic orientation, thinned to 30-40μm in thickness, polished to a flatness of 0.5 μm, and again etched in warm HNO_3. As previously proposed,[12] the orientation and thickness were chosen to provide a single domain in order to minimize stress and to avoid fracture during the MIT.

Silver contacts were deposited on the multidomain, randomly oriented samples in a conventional four-probe arrangement, as shown in Fig. 1. To minimize stresses caused by conventional electrical contacts, an alternative contact arrangement in Fig. 2 was used for the single-domain samples with a well-defined crystallographic orientation. Silver contacts were deposited on both sides of the thin V_2O_3 disks. The sample was placed on a thin copper plate (~50 μm in thickness) and this assembly was then sandwiched between two thin mica sheets (~10 μm in thickness each). A small rectangular window that was cut out of the top sheet of mica permitted electrical contact to be made to the sample with a spherical silver probe. An electrometer with an input impedance exceeding 10^{13} Ω cm was used for the electrical measurements. This technique made it possible to reduce the sample resistance by more than two orders of magnitude and thus, to extend the temperature interval of the measurements. The accuracy of this two-probe technique was verified by comparing the data with those of measurements carried out by the standard four-probe technique, at temperatures overlapping those of this study. The conductivity measurements were taken on first cooling, past the phase transition.

III. RESULTS AND DISCUSSION

Conductivity measurements in the AFI phase taken during the first cooling cycle for single-domain and multidomain

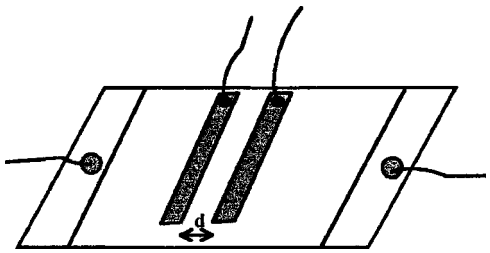

FIG. 1. Conventional four-probe contact arrangement for randomly oriented, multidomain samples.

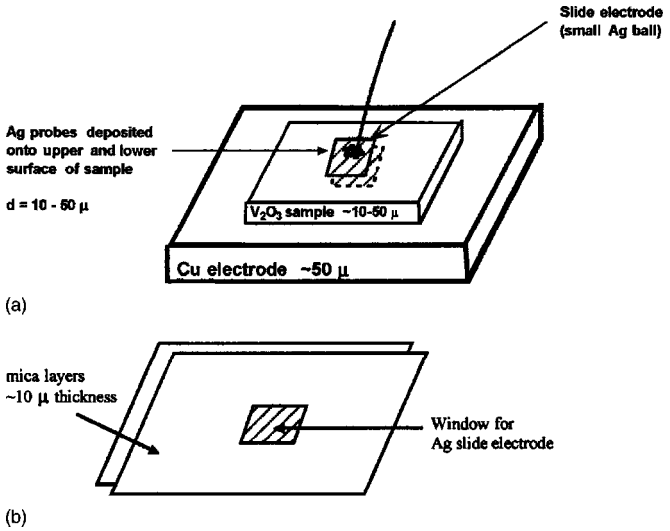

FIG. 2. (a) Alternative two-probe contact arrangement for single-domain samples of well-defined orientation. (b) Mica envelope for insertion of two-probe assembly.

V_2O_3 samples are shown in Fig. 3 as a plot of $\log_{10}\sigma$ versus T. For single-domain samples this plot is linear. The measured conductivity for the multidomain sample is of the same order of magnitude, but the $\log_{10}\sigma$ versus T plot is nonlinear, over the entire temperature range of the measurements.

Conductivity measurements of the multidomain sample are shown in Fig. 4 as a plot of $\log_{10}\sigma$ versus $T^{-1/4}$. In the range $150 \geqslant T \geqslant 75$ K ($0.285 \leqslant 1/T^{1/4} \leqslant 0.335$) the data fall on a straight line, in conformity with Mott's variable range law.[13] Between 75 and 65 K ($0.34 \leqslant 1/T^{1/4} \leqslant 0.355$), slight deviations were encountered from Mott's $1/4$ power law, but the variable range law still provided the best overall empirical fit out of all the various theoretical expressions that were tried.

Twinning and domain formation in V_2O_3 are the direct result of the lattice distortion accompanying the MIT and create stresses such as dislocations and cracks at the domain boundaries.[15] The physical properties of V_2O_3 are very sensitive to these mechanical stresses in the AFI phase.[16] Since the dislocations and cracks are randomly distributed, they give rise to potential distortions that result in the observed $\log_{10}\sigma$ versus $T^{-1/4}$ dependence for the two-probe and four-probe multidomain sample measurements.

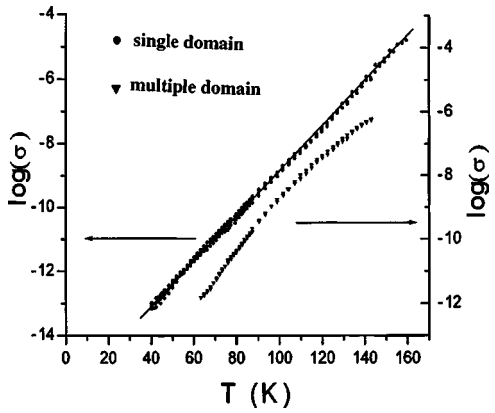

FIG. 3. $\text{Log}_{10}[\sigma\ (\text{ohm-cm})^{-1}]$ vs T plot for multidomain and single-domain V_2O_3 single-crystal samples. Note the difference in scale for the two samples. The right-hand scale holds for multidomain samples.

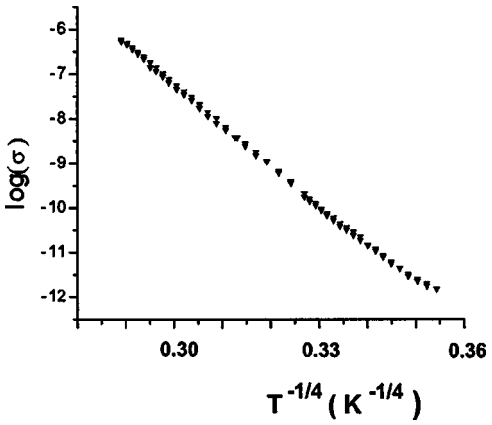

FIG. 4. $\text{Log}_{10}\,\sigma(T)$ vs $T^{-1/4}$ plot for multidomain V_2O_3 single-crystal samples.

The presence of fractures and stresses that accompany the transition mask the correct $\sigma(T)$ dependence, as indicated by the measurement on the single-domain sample, using the modified contact technique.[12,14] These data fall on a straight line of Fig. 3 in the range $160 \geqslant T \geqslant 40$ K. This particular dependence was selected from a large set of empirical functions for $\sigma(T)$ that had been examined, because it provided the best overall fit to the data. The result of this measurement is believed to provide the intrinsic conductivity of unstressed V_2O_3 in the AFI state.

The manner in which thermal lattice vibrations affect the resonance integral leads to the observed linear dependence of $\log_{10}\sigma$ versus T. This can be explained in terms of the theory developed by Tredgold.[17] In this theory, which treats the problem of electron tunneling between nearest neighbors through potential barriers that vary randomly with time, the conductivity is predicted to vary with the temperature as $\ln\sigma \sim T$. This concept was applied only much later to many low-conductivity materials.[18,19]

The random fluctuations of potential arise essentially from the vibration of lattice atoms about their equilibrium positions. We therefore analyzed our data within the framework presented by Bryksin[20,21] for a set of small polarons for which the effect of the displacements of lattice atoms on intersite hopping has been taken into account. These displacements give rise to changes in the wave-function overlap between neighboring atoms. The resonance integral (I) is determined by this overlap. To the first approximation, I varies with the distance (R) covered by the hopping event as $\exp(-\alpha R)$, where α^{-1} is the effective localization radius. In turn, the charge-carrier hopping mobility (μ) is proportional to I^2. For small values of α^{-1}, of the order of the lattice vibration amplitude (ρ), one expects I^2 to depend linearly on ρ, as well as on the temperature dependence of the hopping conductivity.[17] With an I^2 dependence on ρ, it is permissible to replace I^2 by $\langle I^2\rangle$, where the angular brackets represent phonon averaging, via renormalization through the Debye-Waller factor,

$$\langle I^2\rangle = I^2 \exp(2\alpha^2\langle\rho^2\rangle), \tag{1}$$

where $\langle\rho^2\rangle$ is the mean-square displacement of the lattice atoms at temperature T. In the above equation we note that $I \sim \exp(-\alpha R_o)$, where R_o is the distance covered by the hopping event, averaged over the phonon distribution. At high temperatures $\langle\rho^2\rangle$ is proportional to k_BT (where k_B is Boltzmann's constant), so that the associated renormalization of I gives rise to a distinct temperature dependence of the conductivity,[21] namely,

$$\sigma = \frac{\sqrt{\pi} n e^2 a^2 I^2}{h\sqrt{E_a}(k_BT)^{3/2}} \exp[-E_a/k_BT + k_BT/\epsilon], \tag{2}$$

where a is the lattice constant, E_a is the energy required to execute an electron hop, n is the charge-carrier density, e is the magnitude of the electron charge, h is Planck's constant, and ϵ is a quantity with the dimensions of energy. At high temperatures such that $2k_BT > \hbar\omega_q$ (where $\hbar = h/2\pi$, and ω_q is the optical-phonon frequency), ϵ is related to the mean-square displacement by

$$\epsilon = k_BT/2\alpha^2\langle\rho^2\rangle. \tag{3}$$

For the temperature interval 160–40 K of our measurements the high-temperature limit $2k_BT > \hbar\omega_q$ is met up to $T = 120$–130 K because the energy of the lowest-frequency optical phonon is $\hbar\omega_q = 2.3\times10^{-2}$ eV.[22] Generally, in electron-phonon interactions the acoustic as well as the optical phonons take part in the scattering process, but at low temperatures only the low-frequency acoustic phonons participate significantly. We now introduce the Einstein approximation, employing a characteristic phonon frequency. Then, the mean-square displacement is given by

$$\langle\rho^2\rangle = 2k_BT/M\omega^2, \tag{4}$$

where M is the mass of the lattice atoms. Examination of Eq. (2) shows that in the high-temperature regime the first exponential factor may be neglected in comparison to the second, whereas the first exponential factor dominates in the low-temperature limit. In the high-temperature regime Eq. (2) may be written in the form

$$\ln(\sigma T^{3/2}) = A + k_BT/\epsilon, \tag{5}$$

where A and ϵ are independent of T.

The results of measurement of the single-domain sample are shown in Fig. 5 as plots of $\ln(\sigma T^{3/2})$ versus T. At high temperature the $T^{3/2}$ factor does not influence the linear character $\ln\sigma \sim T$ but below 60 K the influence of this factor becomes perceptible. Comparison of Figs. 3 and 5 shows that at 50 K there is a slight deviation from a straight line, arising from the term $-E_a/k_BT$ in Eq. (2). The slope of the straight line in Fig. 5 provides a value of $\epsilon = 4.95\times10^{-4}$ eV (7.92×10^{-16} erg). The goodness of fit of Fig. 3 relative to the theoretical foundation of Fig. 5 is only apparent. Ultimately the $\ln\sigma \sim T$ dependence must give way to the $\ln\sigma \sim 1/T$ variation. Our instrumentation did not enable us to reach the lower-temperature range where deviations from linearity in Fig. 3 would have become apparent.

If Eq. (2) is written in the form,

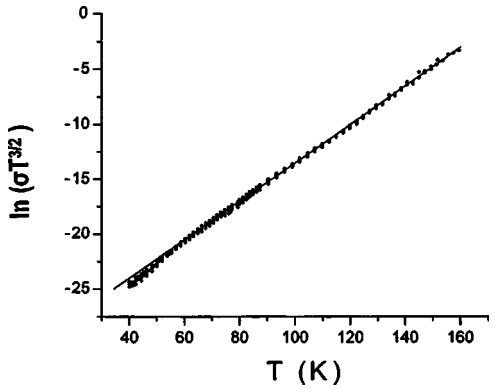

FIG. 5. $\mathrm{Ln}(\sigma T^{3/2})$ vs T plot for single-domain V_2O_3 samples.

$$\ln(\sigma T^{3/2}) - k_BT/\epsilon = A - E_a/k_BT \tag{6}$$

(where $\epsilon = 4.95\times10^{-4}$ eV), then one can estimate for the temperature interval 60–40 K (where the deviation from the straight line of Fig. 5 occurs) a value of $E_a = 8\times10^{-3}$ eV.

Figure 6 shows the temperature dependence of the conductivity of the single-domain sample as a plot of $\ln(\sigma T^{3/2}) + E_a/k_BT$ versus T, with $E_a = 8\times10^{-3}$ eV. One obtains a good linear fit over the entire temperature range, showing that the deviation from the straight line in Fig. 5 arises from the factor E_a/k_BT in Eq. (2). Thus, the high-temperature range over which Eq. (5) is expected to hold, extends down to the region $T = 50$-60 K.

Examination of Eqs. (1)–(3) shows that corrections to the temperature dependence of the conductivity due to thermal vibrations are important only when $(2\alpha^2\langle\rho^2\rangle) \geqslant 1$, i.e., for materials with a very small radius of electron localization that is comparable to the lattice vibration amplitude. From Eq. (3) we can estimate the value of $(2\alpha^2\langle\rho^2\rangle) = 20$ at $T = 120$ K. This means that the effective localization radius is $\alpha^{-1} = (1/3)\ \rho$.

We can estimate the value of the lattice vibration amplitude by using Eq. (4), the atomic mass of vanadium $M = 0.86\times10^{-22}$ g/atom, and characteristic phonon frequency $\omega = 10^{13}$ s^{-1}. At $T = 120$ K one arrives at an estimate of $\rho = 0.2\times10^{-8}$ cm. The small polaron radius of localization ob-

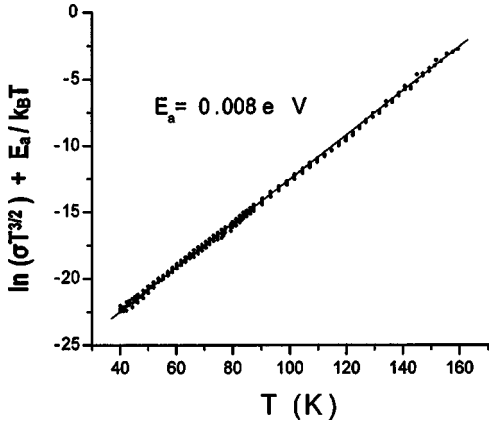

FIG. 6. Plot of $\ln(\sigma T^{3/2}) + E_a/k_BT$ vs T for the single-domain V_2O_3 sample; $E_a = 8\times10^{-3}$ eV.

tained through this analysis is $\alpha^{-1}=0.06\times10^{-8}$ cm, which is smaller than the ionic radius of vanadium and the vibration amplitudes in solids, that tend to be of order 0.2×10^{-8} cm. Such a small value of α^{-1} may make it necessary to regard this quantity as an effective localization length, but a microscopic interpretation requires the development of further theoretical inputs. Of course one could increase the effective localization radius by one order of magnitude on decreasing the assumed characteristic phonon frequency to $\omega=10^{12}$ s^{-1}. The above estimates are rough because we do not know the phonon spectrum of V_2O_3 at low temperature, and because we have applied the relevant equations in a regime where they apply only marginally. Thus, to clarify this situation, additional investigations are required.

IV. CONCLUSIONS

The intrinsic conductivity in the AFI phase of V_2O_3 has been measured using a special experimental setup with a single-domain crystal, free of cracks and mechanical stresses. The result is summarized in Fig. 3 and compared with the conductivity of V_2O_3 where no precautions were taken to maintain the integrity of the sample. The electrical characteristics follow the temperature dependence specified in Eq. (6), which is based on the effect of lattice thermal vibrations on intersite hopping of the charge carriers. This temperature dependence is quite different from that which holds for multidomain samples subject to mechanical stresses. The localization radius of the polarons is of the order of the thermal lattice vibration amplitude.

ACKNOWLEDGMENTS

We wish to thank Professor W. Bryksin, of the Physico-Technical Institute Academy of Sciences of Russia for fruitful discussions during the preparation of this paper. V.N.A. was supported by Grant No. 10002-251/OFN-03/049-054/020703-950 of the Russian Academy of Sciences. J.M.H. and P.A.M. were supported by Grant No. DMR96-12130 of the National Science Foundation.

*Present address: 900 Walt Whitman Road, Melville, NY 11747.

[1] J. G. Austin, C. E. Turner, Philos. Mag. **19**, 2914 (1969).
[2] K. Kosuge, J. Phys. Soc. Jpn. **22**, 551 (1967).
[3] J. G. Austin and C. E. Turner, Philos. Mag. **19**, 9393 (1969).
[4] D. B. McWhan, T. M. Rice, and J. P. Remeika, Phys. Rev. Lett. **23**, 1384 (1969).
[5] A. Jayaraman, D. B. McWhan, J. P. Remeika, and P. D. Dernier, Phys. Rev. B **2**, 3751 (1970).
[6] D. B. McWhan, A. Menth, and J. P. Remeika, J. Phys. (Paris) **32**, C1-1079 (1971).
[7] M. Pouchard and J. C. Launay, Mater. Res. Bull. **8**, 95 (1973).
[8] N. Kimizuka, M. Ishii, M. Saeki, M. Nakano, and M. Nakahira, Solid State Commun. **12**, 43 (1973).
[9] H. Kuwamoto, J. M. Honig, and J. Appel, Phys. Rev. B **22**, 2626 (1980).
[10] S. A. Carter, T. F. Rosenbaum, M. Lu, H. M. Jaeger, P. Metcalf, J. M. Honig, and J. Spalek, Phys. Rev. B **49**, 7898 (1994).
[11] P. A. Metcalf and J. M. Honig, Curr. Top. Cryst. Growth Res. **2**, 445 (1995).
[12] V. N. Andreev and F. A. Chudnovskii, Sov. Phys. Solid State **17**, 1966 (1976).
[13] N. F. Mott, Philos. Mag. **19**, 835 (1969).
[14] F. A. Chudnovskiy, V. N. Andreev, V. S. Kuksenko, V. A. Piculin, D. I. Frolov, P. A. Metcalf, and J. M. Honig, J. Solid State Chem. **133**, 430 (1997).
[15] P. D. Dernier and M. Marezio, Phys. Rev. B **2**, 3771 (1970).
[16] D. B. McWhan, A. Menth, J. P. Remeika, W. F. Brinkman, and T. M. Rice, Phys. Rev. B **7**, 1920 (1973).
[17] R. H. Tredgold, Proc. Phys. Soc. London **80**, 807 (1962).
[18] I. Shiozaki, C. M. Hurd, S. P. McAlister, W. R. McKinnon, and P. Strobel, J. Phys. C **14**, 4641 (1981).
[19] C. M. Hurd, J. Phys. C **18**, 6484 (1985).
[20] W. Bryksin and S. D. Khanin, Fiz. Tverd. Tela (Leningrad) **35**, 2266 (1993).
[21] W. Bryksin, Zh. Eksp. Teor. Fiz. **100**, 1556 (1991).
[22] D. N. Mirlin and I. I. Reshina, Fiz. Tverd. Tela (Leningrad) **19**, 201 (1977).